The Astrophysical Journal Letters, 734:L13 (5pp), 2011 June 10 doi:10.1088/2041-8205/734/1/L13

HYDROGEN GREENHOUSE PLANETS BEYOND THE HABITABLE ZONE

Raymond Pierrehumbert[1] and Eric Gaidos[2]
[1] Department of the Geophysical Sciences, University of Chicago, Chicago, IL 60637, USA; rtp1@geosci.uchicago.edu
[2] Department of Geology and Geophysics, University of Hawaii at Manoa, Honoulu, HI 96822, USA; gaidos@hawaii.edu
Received 2011 April 3; accepted 2011 April 29; published 2011 May 19

ABSTRACT

We show that collision-induced absorption allows molecular hydrogen to act as an incondensible greenhouse gas and that bars or tens of bars of primordial H_2–He mixtures can maintain surface temperatures above the freezing point of water well beyond the "classical" habitable zone defined for CO_2 greenhouse atmospheres. Using a one-dimensional radiative–convective model, we find that 40 bars of pure H_2 on a three Earth-mass planet can maintain a surface temperature of 280 K out to 1.5 AU from an early-type M dwarf star and 10 AU from a G-type star. Neglecting the effects of clouds and of gaseous absorbers besides H_2, the flux at the surface would be sufficient for photosynthesis by cyanobacteria (in the G star case) or anoxygenic phototrophs (in the M star case). We argue that primordial atmospheres of one to several hundred bars of H_2–He are possible and use a model of hydrogen escape to show that such atmospheres are likely to persist further than 1.5 AU from M stars, and 2 AU from G stars, assuming these planets have protecting magnetic fields. We predict that the microlensing planet OGLE-05-390Lb could have retained an H_2–He atmosphere and be habitable at ∼2.6 AU from its host M star.

Key words: astrobiology – planetary systems

Online-only material: color figures

1. INTRODUCTION

In the circumstellar habitable zone (HZ), an Earth-like planet has surface temperatures permissive of liquid water (Hart 1979). The HZ is typically calculated assuming an H_2O–CO_2 greenhouse atmosphere. At its inner edge, elevated water vapor leads to a runaway greenhouse state; at the outer edge, CO_2 condenses onto the surface. The HZ of the Sun is presently 0.95–2 AU but is much more compact around less-luminous M dwarfs (Kasting et al. 1993). Most reported Earth-size exoplanets are well starward of the HZ because the Doppler and transit detection techniques are biased toward planets on close-in orbits (Gaidos et al. 2007). The *Kepler* mission can detect Earth-size planets in the HZ of solar-type stars (Koch et al. 2010; Borucki et al. 2011), but these cannot be confirmed by Doppler. In contrast, the microlensing technique, in which a planet around a foreground gravitational lensing star breaks the circular symmetry of the geometry and produces a transient peak in the light curve of an amplified background star, is sensitive to planets with projected separations near the Einstein radius of their host star, e.g., ∼3.5 AU for a solar mass. Surveys have found planets as small as 3 $M_\oplus$ (Bennett et al. 2008) and projected separations of 0.7–5 AU (Sumi et al. 2010). Most microlensing-detected planets orbit M dwarf stars as these dominate the stellar population. The Einstein radius of these stars is well outside the classical HZ (Sumi et al. 2010; Kubas et al. 2010) but coincides with the "ice line" where Neptune-mass or icy super-Earth planets may form (Gould et al. 2010; Mann et al. 2010).

The effective temperatures of microlensing planets around M stars will be below the condensation temperature of all gases except for H_2 and He. These mono- and di-atomic gases lack the bending and rotational modes that impart features to the infrared absorption spectra of more complex molecules. At high pressure, however, collisions cause H_2 molecules to possess transient dipole moments and induced absorption. The resulting greenhouse effect can considerably warm the surface. Stevenson (1999) conjectured that "free-floating" planets with thick H_2–He atmospheres might maintain clement conditions without the benefit of stellar radiation. Around a star, an H_2–He atmosphere might admit visible light to the surface: these planets could, in principle, host photosynthetic life.

We demonstrate that H_2 and He alone can maintain surface temperatures above the freezing point of water on Earth-mass to super-Earth-mass planets beyond the HZ. In Section 2, we describe calculations of a radiative–convective atmosphere and its transmission of light; results are given in Section 3. In Section 4, we estimate the amount of H_2 gas that a planet may accrete from its nascent disk, and the amount lost back to space. Finally, we discuss the effects of other gases and a candidate H_2 greenhouse planet detected by microlensing (Section 5).

2. CALCULATION OF RADIATIVE FLUXES AND SURFACE TEMPERATURE

Surface temperatures were computed using a one-dimensional radiative–convective model. For pure H_2 and H_2–He atmospheres, the infrared opacity due to collision-induced absorption is from Borysow (2002). (Effects of additional greenhouse gases are discussed in Section 5.) Thermal infrared fluxes for any given temperature profile were computed using the integral form of the solution to the non-scattering Schwarzschild equations, while the planetary albedo and absorption profile of incoming stellar radiation were computed using a two-stream scattering code including the effects of continuum absorption and Rayleigh scattering. The incoming stellar flux was modeled as blackbodies at 3500 and 6000 K for M and G stars, respectively. The calculations were independently performed in wavenumber bands of width 10 cm^{-1} over 10–16490 cm^{-1}. The atmosphere was assumed not to absorb at higher wavenumbers ($\lambda < 606$ nm), although Rayleigh scattering of incoming stellar radiation was still considered. Continuum absorption is a smooth function of wavenumber, obviating the need for a statistical model within each band. Convection

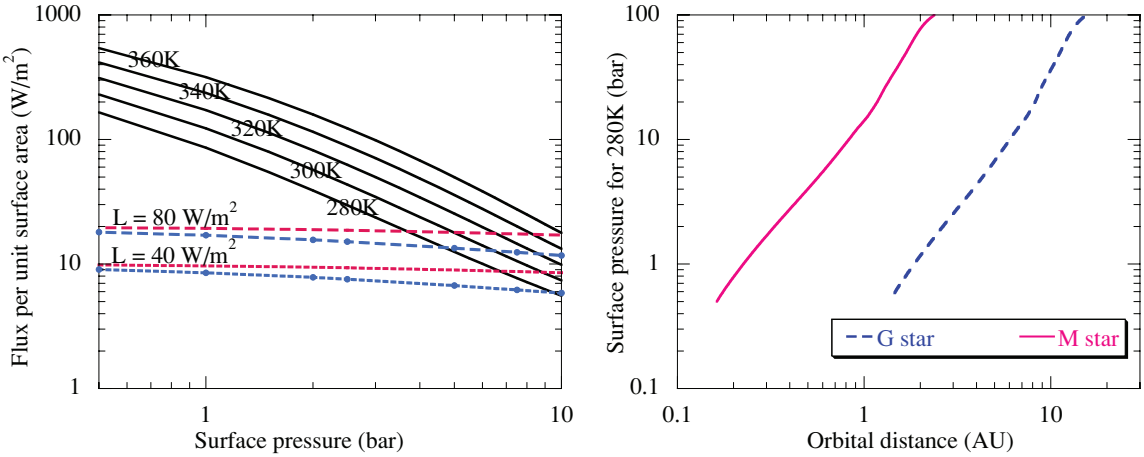

Figure 1. Left panel: determination of surface temperature from the top-of-atmosphere radiation budget. Solid curves show the OLR (infrared emission to space) as a function of surface pressure for the various surface temperatures indicated on the curves. Pairs of dashed lines give the absorbed solar radiation for stellar constant 40 W m^{-2} (short dashes) and 80 W m^{-2} (long dashes). The upper curve in each pair is for an M star spectrum, while the lower is for a G star. Right panel: surface pressure required to maintain 280 K surface temperature as a function of radius of a circular orbit. Results are given for an M star (0.013 times solar luminosity) and a G star (solar luminosity). All calculations were carried out for a pure H_2 atmosphere on a planet with surface gravity 17 m s^{-2}. Planetary albedos were computed assuming zero surface albedo.

(A color version of this figure is available in the online journal.)

was modeled by adjustment to the adiabat appropriate for a dry H_2–He composition (but see Section 5). The adiabat was computed using the ideal gas equation of state with constant specific heat.

In selected cases up to 10 bar surface pressure p_s, the full radiative–convective model was time stepped to equilibrium. The atmosphere was found to consist of a deep convective troposphere capped by a nearly isothermal stratosphere. Absorption of incoming stellar radiation slightly warms the stratosphere, but does not create an Earth-like temperature inversion because the pressure dependence of absorption means that most absorption of stellar radiation and heating occurs at low altitude or at the surface. The tropopause occurs at a pressure level of $\leqslant$170 mbar, producing an optically thin stratosphere that has little effect on infrared cooling to space. For $p_s = 1$ bar, the formation of the stratosphere cools the surface by only 3 K relative to a calculation in which the entire temperature profile is adiabatic. The slight effect becomes even less consequential as p_s and the infrared optical thickness of the atmosphere increases (Pierrehumbert 2010, Chapter 4). Therefore, we used the computationally efficient "all troposphere" approximation, in which the temperature profile is set to the adiabat corresponding to an assumed surface temperature T_g.

The radiation code calculates the corresponding infrared flux to space OLR(T_g, p_s) (outgoing longwave radiation) and planetary albedo $\alpha(T_g, p_s)$. T_g is obtained from the balance

$$\mathrm{OLR}(T_g, p_s) = \frac{1}{4}(1 - \alpha(T_g, p_s))L, \qquad (1)$$

where L is the stellar constant evaluated at the planet's orbit (the analog of Earth's solar constant $L_\odot$).

3. CLIMATE MODEL RESULTS

3.1. Minimum Surface Pressure to Maintain Surface Liquid Water

We present results for a 3 $M_\oplus$ rocky planet with surface gravity $g = 17$ m s^{-2} (Seager et al. 2007). Gravity enters the calculation of OLR only in the combination p_s^2/g; the results can be applied approximately to other values of g by scaling p_s. Scaled results will diverge slightly from the correct values because Rayleigh scattering depends on p_s/g, whence albedo scales differently from OLR. Figure 1 (left panel) illustrates the energy balance for a pure H_2 atmosphere. OLR computed with the all-troposphere approximation is shown as a function of p_s for different values of T_g, together with curves of absorbed stellar radiation for G and M star cases with stellar constants $L = 40$ W m^{-2} and $L = 80$ W m^{-2}, respectively. Equilibria are represented by the intersections between OLR curves and absorbed stellar radiation curves. The absorbed stellar radiation decreases more rapidly with p_s for G stars than for M stars because the greater shortwave radiation in the former case leads to more Rayleigh scattering, whereas the latter is dominated by absorption. For $L = 40$ W m^{-2} (somewhat less than Jupiter's insolation), $p_s = 10$ bar is sufficient to maintain a surface temperature of 280 K about a G star; around an M star, only 7 bars is required.

Figure 1 (right panel) also shows the minimum p_s required to maintain $T_g = 280$ K as a function of the orbital distance. We use 280 K as a criterion because an ocean world whose global mean temperature is too near freezing is likely to enter a "snowball" state (Pierrehumbert et al. 2011). The required pressure is higher around M stars because a greater greenhouse effect is needed to compensate for the lower luminosity. For an early M-type star with luminosity 1.3% of the Sun, 100 bars of H_2 maintains liquid surface water out to 2.4 AU; around a G star, these conditions persist to 15 AU. Cases requiring >20 bars are speculative because the maintenance of a deep convective troposphere, when so little stellar radiation reaches the surface, is sensitive to small admixtures of strongly shortwave-absorbing constituents.

Our results are not appreciably affected by the formation of a stratosphere. The stratosphere in these atmospheres is essentially transparent to incoming stellar radiation and heated mainly by absorption of upwelling infrared radiation. As expected for a gas with frequency-dependent absorptivity, the stratospheric temperature is somewhat (few K) below the gray-gas skin temperature $T_{\mathrm{eff}}/2^{1/4}$, where $\sigma T_{\mathrm{eff}}^4 = \mathrm{OLR} = \frac{1}{4}(1-\alpha)L$ (Pierrehumbert 2010, chapter 4).

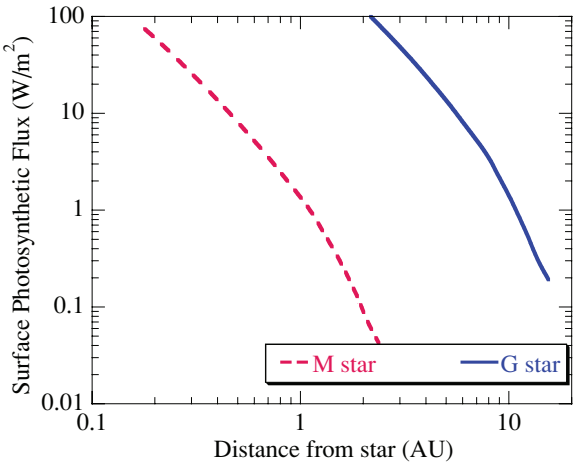

Figure 2. Flux in the photosynthetically active band (400–700 nm) reaching the surface at the substellar point as a function of distance from a G or an M host star. The flux is calculated assuming an H_2 atmosphere with surface pressure sufficient to maintain 280 K surface temperature at each distance.

(A color version of this figure is available in the online journal.)

3.2. Photosynthetic Active Radiation at the Surface

Starlight is a potential energy source for life, so we consider whether the stellar flux reaching the surface is sufficient to sustain photosynthesis. Most terrestrial photosynthetic organisms use light in the $\lambda = 400$–700 nm range. The flux to sustain half-maximum growth rate for many cyanobacteria is ~ 1 W m^{-2} (Carr & Whitton 1982; Tilzer 1987), and an anoxygenic green sulfur bacterium can use a flux of 3×10^{-3} W m^{-2} (Manske et al. 2005). Planets on more distant orbits experience less stellar irradiation and require a thicker atmosphere to maintain surface liquid water, which reduces transmission of light to the surface. For a pure H_2 atmosphere, transmission in photosynthetically active radiation (PAR) is limited by Rayleigh scattering and differs slightly for M versus G star spectra. The main difference is that G stars have higher luminosity, requiring less atmosphere to maintain liquid water at a given orbital distance, and a higher proportion of their output is PAR. Figure 2 shows surface PAR at the substellar point as a function of orbital distance for a minimum pure H_2 atmosphere to maintain 280 K. Hydrogen greenhouse planets as far as 10 AU from a G star or 1 AU from an M star could sustain cyanobacteria-like life; distances of tens of AU or several AU, respectively, still permit organisms like anoxygenic phototrophs.

4. ORIGIN AND LOSS OF H–He ATMOSPHERES

A body whose Bondi radius (at which gravitational potential energy equals gas enthalpy) exceeds its physical radius will accumulate gas from any surrounding disk. The critical mass is less than a lunar mass and protoplanets may acquire primordial atmospheres of H_2 and He, as well as gases released by impacts (Stevenson 1982). Earth-mass planets will not experience runaway gas accretion and transformation into gas giants (Mizuno 1980). The atmospheres of accreting Earth-mass planets will probably be optically thick and possess an outer radiative zone (Rafikov 2006). If the gas opacity is supplied by heavy elements and is pressure independent, the atmosphere mass is inversely proportional to the accretion luminosity (Stevenson 1982; Ikoma & Genda 2006; Rafikov 2006). In the "high accretion rate" case (planetesimals are strongly damped by gas drag), the surface pressure will be $1.2a^{1.5}(M_p/M_\oplus)$ bar, where a is the orbital semimajor axis in AU and M_p is the planet mass. In the "intermediate accretion rate" case (gas drag is unimportant), the surface pressure will be $16a^2(M_p/M_\oplus)$ bar (Rafikov 2006). At 3 AU, the predicted timescales for these two phases of accretion are $\sim 10^6$ and 10^7 yr, respectively, and bracket the lifetime of gaseous disks (Haisch et al. 2001; Evans et al. 2009). Thus, primordial atmospheres with surface pressures of one to several hundred bars are plausible. Hydrogen is also released during the reaction of water with metallic iron (Elkins-Tanton & Seager 2008).

Giant impacts may erode the proto-atmosphere, but not completely remove it (Genda & Abe 2003, 2004), although the mechanical properties of an ocean may amplify such effects (Genda & Abe 2005). Instead, the low molecular weight μ of atomic H makes it susceptible to escape to space through heating of the upper atmosphere by extreme ultraviolet (EUV) radiation and stellar wind. We examine EUV-driven escape of atomic H from a planet of radius r_p using a thermal model of an H- or H_2-dominated upper atmosphere, assuming that the escape rate is not limited by H_2 dissociation. The upper boundary is at the exobase where H escapes, and the lower boundary is where eddy diffusivity becomes important (in essence, the homopause). At the homopause, the number density is taken to be $n = 10^{19}$ m^{-3} (Yamanaka 1995), and the temperature is set to the stratosphere temperatures predicted by the radiative–convective model (see Section 3). The exobase occurs at an altitude h_e where the cross section for collisions with molecular hydrogen is ~ 1, i.e., at a column density $N = 2.3 \times 10^{19}$ m^{-2}. The exobase temperature T_e and Jeans parameter $\lambda = GM_p\mu/((r_p + h_e)kT_e)$ are calculated by balancing the globally averaged EUV heating $q_{\rm EUV}$ with heat lost to conduction, radiative cooling, and escape. At $\lambda > 2.8$, we use the Jeans escape rate (in surface pressure per unit time)

$$\phi = \frac{(GM_p)^2\mu}{(r_p + h_e)^4}\sqrt{\frac{\mu}{2\pi kT_e}}N_e(1+\lambda)e^{-\lambda}, \quad (2)$$

where N_e is the number density at the exobase. For Jeans escape, we assume that H is the escape component and that H_2 is efficiently dissociated below the exobase; this maximizes the escape rate. When $\lambda \leqslant 2.8$, marking the transition to hydrodynamic escape (Volkov et al. 2010), we assume that escape is energy limited:

$$\phi = q_{\rm EUV}\frac{(r_p + h_t)^2}{r_p^3}, \quad (3)$$

where h_t is the altitude where EUV is absorbed (the thermosphere), and the right-hand factor accounts for thermal expansion.

All EUV ($\lambda < 912$ Å) is assumed to be absorbed in a layer at $N = 2.3 \times 10^{19}$ m^{-2}. Lyα radiation resonantly scatters at higher altitudes ($N \sim 1 \times 10^{17}$ m^{-2}) but, in the absence of an absorber such as atomic oxygen, will escape before being thermalized (Murray-Clay et al. 2009).

For given exobase and homopause temperatures, the temperature profile is calculated downward to its maximum at the thermosphere and then to the homopause, assuming a mean μ of 3.1 (appropriate for H_2+He in a solar proportion). The exobase temperature is adjusted until the correct value of n at the homopause is reached. Cooling from the escape of H at the exobase, the adiabatic upward motion of gas in the atmosphere to maintain steady state, and the collision-induced opacity of H_2 (Borysow et al. 1997; Borysow 2002) are included. We use

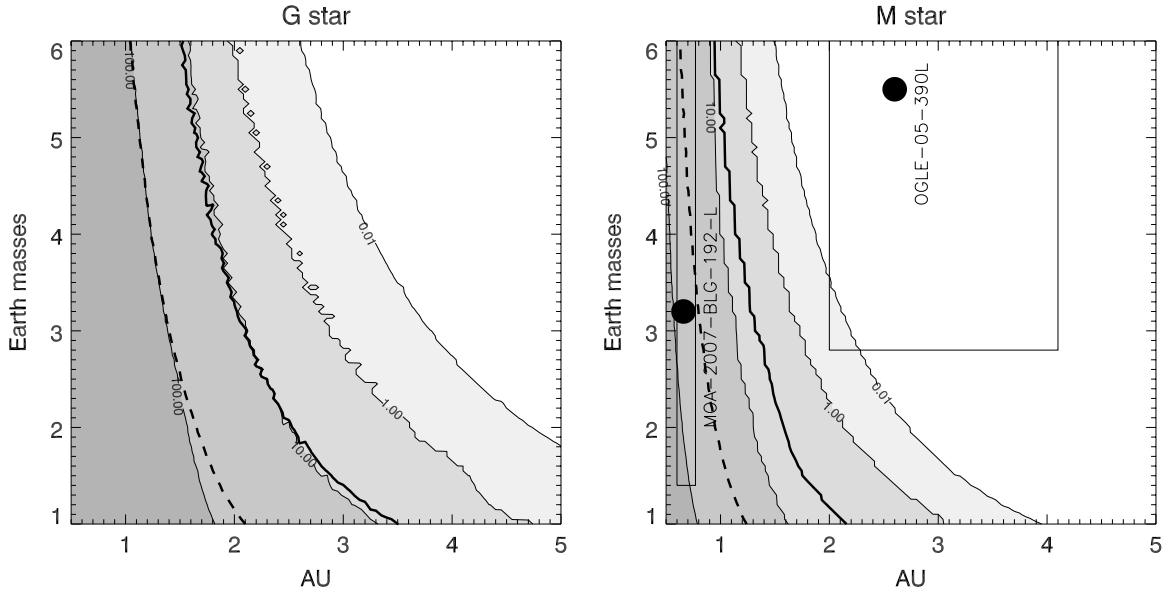

Figure 3. EUV-driven atmospheric escape (bars) at an age of 4.5 Gyr as a function of planet mass and distance from a G star (left) or an M star (right). The heavy solid line is where mass loss equals the estimated mass of proto-atmosphere acquired by a planet during its early phase of oligarchic growth (high rate of planetesimal accretion) and the heavy dashed line is the same for the case of the late phase of oligarchic growth (intermediate rate of planetesimal accretion). See the text for details. Two microlensing-detected super-Earth-mass planets are plotted, with the boxes representing the undercertainties in their parameters.

a thermal conductivity $k \approx 0.0027T^{0.73}$ W m^{-1} K^{-1} based on Allison & Smith (1971). We adopt $q_{\rm EUV} = 1.5 \times 10^{-4}$ W m^{-2} at 1 AU from a 4.5 Gyr old G star (Watson et al. 1981). This is the current solar incident EUV flux of 1.67×10^{-3} W m^{-2} for $\lambda < 900$ Å (Hinteregger et al. 1981; Del Zanna et al. 2010) times a 30% heating efficiency (Watson et al. 1981). EUV is scaled to different ages and M stars assuming proportionality to soft X-ray flux (Penz et al. 2008; Penz & Micela 2008).

At sufficiently high EUV flux, the atmosphere expands to the scale of the planet, gravity at the exobase decreases, no steady-state solution to the temperature profile exists, and $\lambda < 2.8$. We presume this to correspond to hydrodynamic escape, fix the temperature structure at its last state consistent with Jeans escape, and use the energy-limited escape rate (Equation (3)). Additional H may escape as a result of interaction with the stellar wind (Lammer et al. 2007).

We calculate the total atmosphere lost by 4.5 Gyr for planets around G and M dwarf stars (Figure 3). Significant atmospheric loss usually ceases by ∼2 Gyr. Planets around M dwarfs, with their lower X-ray luminosities, can retain their H_2–He atmospheres close to the star. However, these stars, especially those of mid- to late-M spectral type, may vary greatly in their EUV flux (Reiners & Basri 2008; Browning et al. 2010).

5. DISCUSSION

Effects of other gases. The addition of He to the pure H_2 atmospheres considered above would warm the surface by somewhat less than the effect of adding the same number of H_2 molecules, because the collision-induced-absorption coefficients for H_2–He collision are generally weaker than those for H_2–H_2 (Borysow et al. 1988) and because He–He collisions do not contribute. Addition of He also makes the adiabat steeper and the surface warmer relative to the pure H_2 case, but for a 10% He concentration the extra warming is no more than 1 K.

The warming provided by the H_2 greenhouse permits other greenhouse gases to be stable against complete condensation, notably CO_2, H_2O, NH_3, and CH_4. For the distant orbits of interest in this Letter, the effective radiating temperature occurs in the upper troposphere and is ∼60 K for a planet 2 AU from an M star. The low saturation vapor pressure at this temperature confines the gases to lower altitudes, where they add little to the greenhouse effect. Even at 100 K, the saturation vapor pressures of CO_2, H_2O, and NH_3 are all <0.02 Pa. CH_4, with a vapor pressure of 0.338 bar at 100 K, is most likely to exert a modest additional warming effect.

The condensible gases also affect climate through latent heat release, which makes the adiabat less steep and reduces the surface temperature. Because of the heat capacity of the thick H_2 atmosphere, the effect on the adiabat is slight, amounting to, for example, a 3 K surface cooling for an H_2O saturated atmosphere in 5 bars of H_2. It is much less for thicker atmospheres. Instead, the main effect of condensible constituents would be to form tropospheric clouds, which would increase the albedo and hence increase the H_2 pressure needed to maintain habitability. A quantitative treatment of clouds is outside the scope of this Letter.

Cold cases. Two "super-Earth-"mass planets detected by microlensing are plotted in Figure 3(b). MOA-2007-BLG-192Lb orbits ∼0.7 AU from a very late type M dwarf. It has an effective temperature of 40–50 K, below the condensation temperature of all gases except H_2 and He, although N_2 or CO might be volatilized at the substellar point of a synchronously rotating planet (Kubas et al. 2010). We predict that any primordial hydrogen atmosphere has been lost by EUV-driven hydrodynamic escape carrying He and other light volatiles with it. In contrast, more massive OGLE-05-390Lb, which orbits ∼2.6 AU from a mid M-type star but has a similar effective temperature (Beaulieu et al. 2006), may retain a primordial hydrogen atmosphere. This planet could potentially sustain liquid water at its surface and may represent potentially ocean-bearing planets to be revealed by future microlensing surveys (Beaulieu et al. 2008; Bennett et al. 2010).

All planets smaller than Neptune detected by *Kepler* or Doppler orbit within the zone where hydrogen escape is predicted to be efficient. Gliese 581d ($\geqslant 6M_\oplus$, 0.2 AU) is in this

category; though it may lie within the classic HZ (Wordsworth et al. 2010; von Paris et al. 2010; Hu & Ding 2011). Larger, transiting planets such as GJ 436b (22 $M_\oplus$) have retained a low molecular-weight envelope despite their proximity to their parent stars, perhaps due to their high gravity and migration from further out in the primordial nebula. Should the *Kepler* mission be extended (∼6 yr), planets at 1.5–2 AU, the inner boundary where a hydrogen atmosphere is retained (Figure 3), could be confirmed with three transits. Measuring mass would be at the limit of current Doppler technology (radial velocity amplitude $\leqslant 1$ m s^{-1}), but spectra obtained during transits might reveal any H_2-rich atmosphere.

The effects of life. These habitable worlds may nurture the seeds of their own destruction, on account of the chemical disequilibrium between an H_2-dominated atmosphere and (we presume) a comparatively oxidizing silicate mantle. If the planet's tectonics supports CO_2 outgassing as is the case for Earth, then methanogens could deplete the H_2 atmosphere by combining it with CO_2 to produce CH_4. The O_2 produced by cyanobacteria would similarly consume H_2 and convert the atmosphere to organic carbon and water. Either case would eventually cause a freezeout of the atmosphere, in the absence of some biotic or abiotic process that regenerates H_2.

This research was supported by NASA grant NNX10AQ36G and was inspired by discussions between E.G., R.P., Scott Gaudi, and Sara Seager at the Aspen Institute for Physics.

REFERENCES

Allison, A. C., & Smith, F. J. 1971, At. Data Nucl. Data Tables, 3, 371
Beaulieu, J., Kerins, E., Mao, S., & Bennett, D. 2008, arXiv:0808.0005B
Beaulieu, J.-P., et al. 2006, Nature, 439, 437
Bennett, D., et al. 2010, arXiv:1012.4486
Bennett, D. P., et al. 2008, ApJ, 684, 663
Borucki, W. J., et al. 2011, arXiv:1102.0541, 1
Borysow, A. 2002, A&A, 390, 779
Borysow, A., Frommhold, L., & Birnbaum, G. 1988, ApJ, 329, 509
Borysow, A., Jorgensen, U., & Zheng, C. 1997, A&A, 324, 185
Browning, M. K., Basri, G., Marcy, G. W., West, A. A., & Zhang, J. 2010, AJ, 139, 504
Carr, N. G., & Whitton, B. A. 1982, The Biology of Cyanobacteria (Berkeley, CA: Univ. California Press)
Del Zanna, G., Andretta, V., Chamberlin, P., Woods, T., & Thompson, W. 2010, A&A, 518, A49
Elkins-Tanton, L. T., & Seager, S. 2008, ApJ, 685, 1237
Evans, N. J., et al. 2009, ApJS, 181, 321
Gaidos, E., Haghighipour, N., Agol, E., Latham, D., Raymond, S. N., & Rayner, J. 2007, Science, 318, 210
Genda, H., & Abe, Y. 2003, Icarus, 164, 149
Genda, H., & Abe, Y. 2004, Lunar Planet. Sci. Conf., 35, abstract no. 1518
Genda, H., & Abe, Y. 2005, Nature, 433, 842
Gould, A., et al. 2010, ApJ, 720, 1073
Haisch, K. E., Jr., Lada, E. A., & Lada, C. J. 2001, ApJ, 553, L153
Hart, M. H. 1979, Icarus, 37, 351
Hinteregger, H. E., Fukui, K., & Gilson, B. R. 1981, Geophys. Res. Lett., 8, 1147
Hu, Y., & Ding, F. 2011, A&A, 526, A135
Ikoma, M., & Genda, H. 2006, ApJ, 648, 696
Kasting, J. F., Whitmire, D. P., & Reynolds, R. T. 1993, Icarus, 101, 108
Koch, D., et al. 2010, ApJ, 713, L79
Kubas, D., et al. 2010, arXiv:1009.5665
Lammer, H., et al. 2007, Astrobiology, 7, 185
Mann, A., Gaidos, E., & Gaudi, B. 2010, ApJ, 719, 1454
Manske, A., Glaeser, J., Kuypers, M., & Overmann, J. 2005, Appl. Environ. Microbiol., 71, 8049
Mizuno, H. 1980, Prog. Theor. Phys., 64, 544
Murray-Clay, R. A., Chiang, E. I., & Murray, N. 2009, ApJ, 693, 23
Penz, T., & Micela, G. 2008, A&A, 479, 579
Penz, T., Micela, G., & Lammer, H. 2008, A&A, 477, 309
Pierrehumbert, R. T. 2010, Principles of Planetary Climate (Cambridge: Cambridge Univ. Press)
Pierrehumbert, R. T., Abbot, D., Voigt, A., & Koll, D. 2011, Annu. Rev. Earth Planet. Sci., 39, 417
Rafikov, R. 2006, ApJ, 648, 666
Reiners, A., & Basri, G. 2008, ApJ, 684, 1390
Seager, S., Kuchner, M., Hier-Majumder, C. A., & Militzer, B. 2007, ApJ, 669, 1279
Stevenson, D. J. 1982, Planet. Space Sci., 30, 755
Stevenson, D. J. 1999, Nature, 400, 32
Sumi, T., et al. 2010, ApJ, 710, 1641
Tilzer, M. 1987, N.Z. J. Mar. Freshwater Res., 21, 401
Volkov, A. N., Johnson, R. E., Tucker, O. J., & Erwin, J. T. 2011, ApJ, 729, L24
von Paris, P., et al. 2010, A&A, 522, A23
Watson, A. J., Donahue, T. M., & Walker, J. C. G. 1981, Icarus, 48, 150
Wordsworth, R., Forget, F., Selsis, F., Madeleine, J., Millour, E., & Eymet, V. 2010, A&A, 522, A22
Yamanaka, M. 1995, Adv. Space Res., 15, 47